Med Chem Res
DOI 10.1007/s00044-017-2099-z

MEDICINAL CHEMISTRY RESEARCH

ORIGINAL RESEARCH

Synthesis and adenosine receptors binding studies of new fluorinated analogues of pyrido[2,3-*d*]pyrimidines and quinazolines

Balakumar Chandrasekaran[1] · Pran Kishore Deb[2] · Sonja Kachler[3] · Raghuram Rao Akkinepalli[1,5] · Raghuprasad Mailavaram[4] · Karl-Norbert Klotz[3]

Received: 31 July 2017 / Accepted: 12 October 2017

Abstract A series of new fluorine containing pyrido[2,3-*d*]pyrimidines and imidazo[1,2-*c*]pyrido[3,2-*e*]pyrimidines along with a series of bioisosteric fluorinated quinazolines were synthesised following appropriate synthetic schemes and characterised by spectral analytical means. X-ray crystal structure of the key precursor **1** (2-amino-3-cyano-4-trifluoro-methyl-6-phenyl-pyridine) was also determined to gain insight into its reactivity. Binding affinity data of all the compounds for adenosine receptors (ARs) showed that pyrido[2,3-*d*]pyrimidine scaffold with free amino (NH_2) group at 2- and 4-position (**2a**) exhibited the maximum binding affinity for hA_3 AR with similar affinity for the hA_1 and somewhat lower affinity for hA_{2A} ARs resulting in a compound with no A_3 selectivity vs. A_1 and moderate selectivity vs. A_{2A} AR (K_i $hA_1 = 0.62$ μM, $hA_{2A} = 3.59$ μM and $hA_3 = 0.42$ μM). Interestingly, the replacement of both the amino groups with carbonyl (C=O) groups (compound **4**) resulted in significantly improved affinity for hA_1 AR but with moderate selectivity against hA_{2A} and hA_3 ARs (K_i $hA_1 = 0.17$ μM, $hA_{2A} = 0.67$ μM and $hA_3 = 0.68$ μM). In case of fluorinated quinazolines, only compound **18a** showed remarkable affinity for hA_1 AR with significant selectivity against hA_{2A} and hA_3 ARs (K_i $hA_1 = 0.73$ μM, $hA_{2A} > 30$ μM and $hA_3 = 9.27$ μM). The preliminary results of these compounds demonstrate that the fluorinated pyrido[2,3-*d*]pyrimidine and imidazo[1,2-*c*]pyrido[3,2-*e*]pyrimidine can be considered as promising scaffolds for further optimisation in search of potential antagonists with better affinity and selectivity towards hA_1 and hA_3 ARs.

Keywords Fluorinated pyrido[2,3-*d*]pyrimidines · Fluorinated quinazolines · Adenosine receptors binding · X-ray crystallography

Electronic supplementary material The online version of this article (https://doi.org/10.1007/s00044-017-2099-z) contains supplementary material, which is available to authorized users.

✉ Pran Kishore Deb
pdeb@philadelphia.edu.jo
prankishore1@gmail.com

✉ Raghuram Rao Akkinepalli
raghumed@gmail.com

[1] Pharmaceutical Chemistry Division, University Institute of Pharmaceutical Sciences and UGC Center of Advanced Study in Pharmaceutical Sciences (UGC-CAS), Panjab University, Chandigarh 160 014, India

[2] Faculty of Pharmacy, Philadelphia University-Jordan, P. O. BOX (1), Philadelphia University 19392, Jordan

[3] Institut für Pharmakologie und Toxikologie, Universität Würzburg, Versbacher Strasse 9, Würzburg 97078, Germany

[4] Pharmaceutical Chemistry Division, Sri Vishnu College of Pharmacy, Vishnupur, Bhimavaram, Andhra Pradesh, India

[5] Present address: National Institute of Pharmaceutical Education and Research (NIPER), Sector 67, S.A.S. Nagar, Mohali, Punjab 160 062, India

Introduction

Adenosine receptors (ARs) belong to the super family of G-protein-coupled receptors (GPCRs) and are classified into four subtypes A_1, A_{2A}, A_{2B}, and A_3 ARs, respectively, all of which exhibit distinct physiological functions (Fredholm et al. 2011). A_1 ARs are mainly present in the brain with minimum levels in the heart, lungs, kidney, adipose tissue, stomach, spleen, and liver (Ribeiro et al. 2002). A_{2A} ARs are highly distributed in blood platelets, striatum, nucleus

Published online: 26 October 2017

accumbens, and olfactory tubercle (Preti et al. 2015), while A_{2B} ARs regulate a varied number of physiological and pathological events that involve lungs, blood vessels, and bladder (Kalla and Zablocki 2009). A_3 ARs are highly expressed in immune cells, lung and liver and at lower densities in heart, aorta and brain (Borea et al. 2009).

Agonists selective for A_1 AR showed antinociceptive activity and are thought to be useful in the treatment of stroke, epilepsy, migraine, pain, cardiac ischemia, and arrhythmias (Cosimelli et al. 2016) while antagonists might be useful in conditions such as cognitive dysfunction associated with ageing, stroke-induced brain damage or neurodegenerative disorders like Alzheimer's disease (AD) (Ribeiro et al. 2002; Baraldi et al. 2008). A_{2A} AR antagonists are being considered as potential therapeutic alternative for the treatment of Parkinson's disease (PD) (Preti et al. 2015). Recent studies reported the use of highly potent and selective antagonists such as ZM241385, SCH58261 and some xanthine derivatives (istradefylline) as pharmacological tools for this receptor subtype (Bahreyni et al. 2017; Dong et al. 2017; Dungo and Deeks 2013; Kazemi et al. 2017; Shook et al. 2011; van Rhee et al. 1996; Wardas et al. 2001). Recently, istradefylline has been approved for marketing in Japan as an anti-PD agent (Venkatesan et al. 2014). Selective A_{2B} antagonists were shown to decrease pain (inflammatory), and are promising candidates for the treatment of asthma (Brown et al. 2008) and diabetes (Kalla and Zablocki 2009; Baraldi et al. 2008). Agonists of the A_3 AR are thought to be useful for the treatment of stroke, lung injury (asthma and COPD), cardiac ischemia, rheumatoid arthritis, and cancer (Borea et al. 2009; Jacobson et al. 2009). The blockade of A_3 ARs could be beneficial for the treatment of glaucoma, stroke, asthma, and renal failure (Borea et al. 2009; Jacobson et al. 2009). During the past years a number of potent and selective AR antagonists have been developed, including xanthines and non-xanthine derivatives (Baraldi et al. 2008). Recently reported AR antagonists under different stages of clinical and pre-clinical trial are presented in Figs. 1 and 2 (Muller and Jacobson 2011).

The derivatives of pyrido[2,3-*d*]pyrimidine have shown remarkable biological and pharmacological activities, in particular for the treatment of various inflammatory conditions such as allergy, arthritis, and asthma (Suhagia et al.

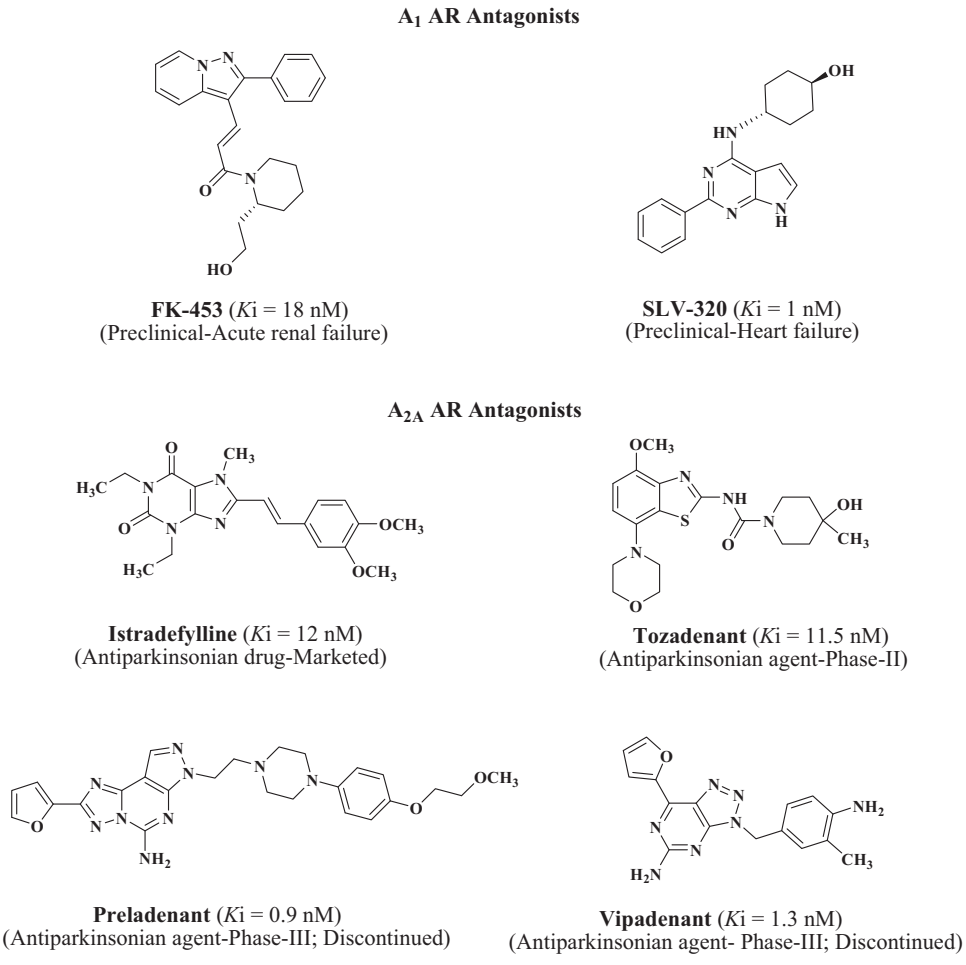

Fig. 1 Recently reported potent hA_1 and hA_{2A} ARs antagonists under different stages of development

2006; Bulicz et al. 2006; Hafez et al. 2008; Nam et al. 2001). Recently, a series of pyrido[2,3-*d*]pyrimidine derivatives have also been reported as selective bicyclic A_{2B} AR antagonists (Eastwood et al. 2011). Thus, it was thought of interest to further explore this pyrido[2,3-*d*]pyrimidine scaffold and evaluate some novel analogues as potent AR antagonists.

Further, quinazolines are considered as bioisosters of pyrido[2,3-*d*]pyrimidines. Quinazoline derivatives exhibited various interesting pharmacological properties including adenosine receptor antagonism (Bertelli et al. 2000; Khan et al. 2014; Smutny et al. 2016). It has been observed that the presence of a fluoro or trifluoromethyl group at a strategic position on the heterocyclic nucleus enhances the activity of a molecule by increasing the lipophilicity (Balakumar et al. 2010). It is interesting to note that the pyrimidine core being part of the endogenous ligand of ARs (adenosine), is a recurrent substructural motif of various heterofused bicyclic and tricyclic AR antagonists. Based on these observations, we earlier designed (Pran Kishore et al. 2011; Balakumar et al. 2017), synthesized and reported a series of triazolothienopyrimidines (Raghu Prasad et al. 2008), 4*H*-pyrimido[2,1-*b*]benzothiazole-2-arylamino-3-cyano-4-ones (Balakumar et al. 2012), pyrido[3,2-*e*][1,2,4]triazolo[1,5-*c*]pyrimidines (Veeraswamy et al. 2013), 2-amino[1,2,4]triazolo[1,5-*c*]quinazolines (Burbiel et al. 2016) as possible ARs antagonists. In continuation to our ongoing efforts, we are reporting a convenient method for the synthesis of trifluoromethyl substituted pyrido[2,3-*d*]pyrimidine analogues from a versatile precursor **1** (2-amino-3-cyano-4-trifluoro-methyl-6-phenyl-pyridine). In order to understand and illustrate the reactivity of this key precursor (**1**), we examined the X-ray crystal structure to gain insight into its structural features. All the newly synthesized

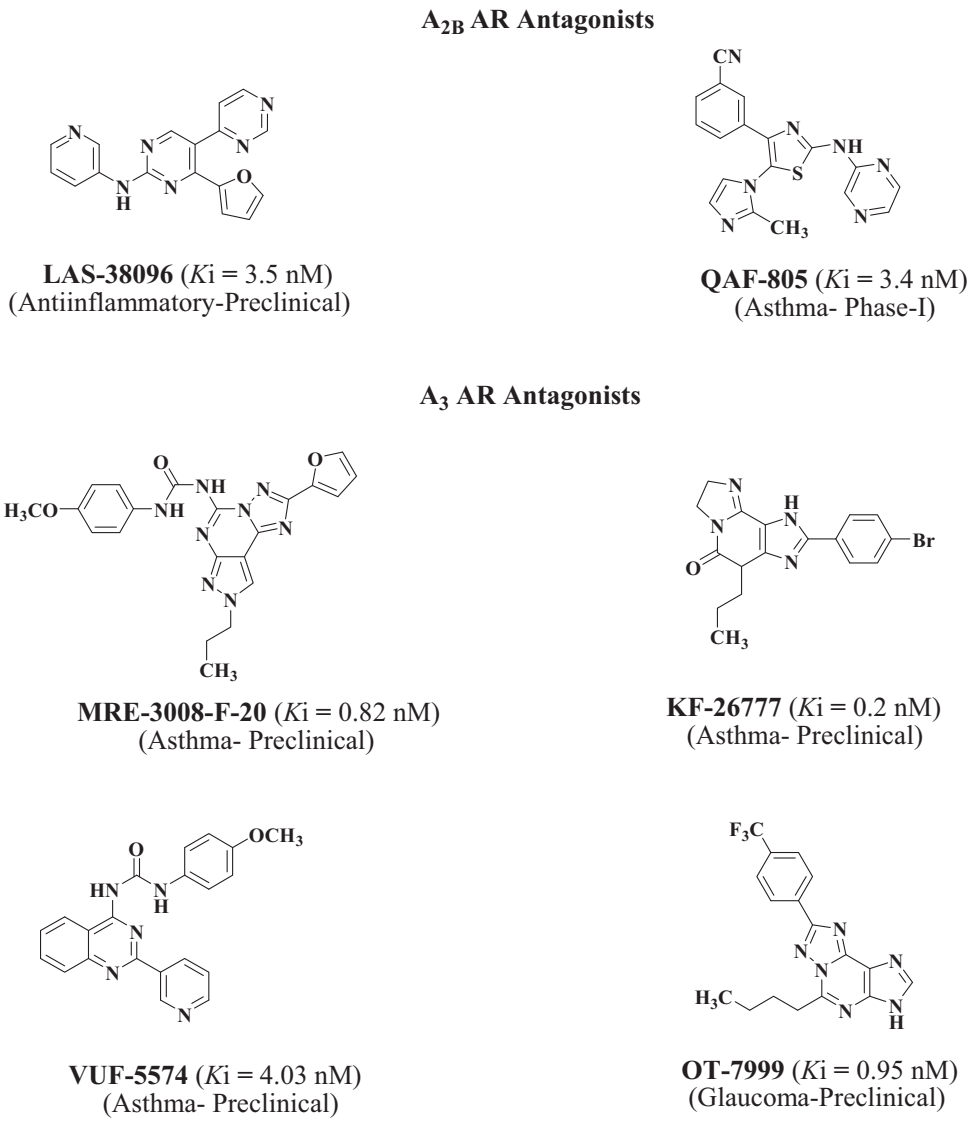

Fig. 2 Recently reported potent hA_{2B} and hA_3 ARs antagonists under different stages of development

compounds (**2a–c, 4, 6a–b**) along with the previously reported bioisosteric fluorinated fused quinazolines (**17a–c** and **18a–c**) have been evaluated for their binding affinity towards all the subtype of ARs.

Experimental

Reactions were routinely monitored by thin layer chromatography (TLC) on silica gel (*precoated F_{254} Merck plates*) and the spots were visualized under UV light (254 nm). Melting points were recorded in open capillaries on *LABINDIA* melting point apparatus and were uncorrected. IR spectra were recorded on *Perkin Elmer FT-IR* Spectrometer (Spectrum RX I) using KBr pellet technique. ^{1}H and ^{13}C NMR spectra were determined in $CDCl_3$ or DMSO-d_6 with a *Bruker Avance II* [400 MHz (^{1}H) and 100 MHz (^{13}C)] spectrometer and signals were recorded in parts per million (δ) downfield from tetramethylsilane as an internal standard. Mass spectra (ESI) were recorded on *Waters Micromass Q-TOF Micro*. *Silica gel* (60–120 mesh) was used for column chromatography. The X-ray crystallographic study was performed for precursor **1**. All measurements were performed on an *Oxford X Calibur Mova* diffractometer using graphite-monochromated MoK_α radiation ($\lambda = 0.71069$ Å) and equipped with a CCD detector.

General procedure for the synthesis of compounds (2a–c)

Dried and pulverized guanidine (0.354 g)/thiourea (0.456 g)/urea (0.36 g) [6 mmol] was added to a solution prepared by dissolving sodium metal (0.138 g, 6 mmol) in absolute ethanol (20 mL) and the mixture was stirred vigorously at 25 °C for 30 min before adding the precursor **1** (0.789 g, 3 mmol). The resulting mixture was heated under reflux for 48–50 h. After completion of the reaction (monitored by TLC), the mixture was poured on to crushed ice, the solid separated was filtered, washed with water. The crude product was dried and purified through column of silica gel (60–120 mesh) using *n*-hexane/ethyl acetate (4:1) as eluent.

*7-Phenyl-5-(trifluoromethyl)-pyrido[2,3-*d*]pyrimidin-2,4-diamine **(2a)***

White solid, yield: 68%, M.P.: 226–228 °C, IR: 3399, 3220, 2926, 1582, 1458, 1371, 1260, 1177, 1132 cm^{-1}; ^{1}H NMR (DMSO-d_6, 400 MHz) δ 6.27 (*s*, 2H, NH$_2$), 7.32 (*s*, 1H, Ar–H), 7.43–7.53 (*m*, 3H, Ar–H), 7.75 (*s*, 1H, NH), 8.04–8.12 (*m*, 2H, Ar–H and 1H, NH) ppm; ^{13}C NMR (DMSO-d_6, 100 MHz,) δ 103.78, 113.35, 124.36, 126.60, 128.83, 129.51, 130.46, 135.07, 137.48, 155.60, 156.41, 166.67 ppm; MS (ESI): *m/z* (%) = 306.1 (15) $[M + H]^+$, 265.0 (100) $[M^+ - 42]$. Elemental analysis: calcd. For $C_{14}H_{10}F_3N_5$: C, 55.08; H, 3.30; N, 22.94%. Found: C, 55.14; H, 3.36; N, 22.87%.

*4-Amino-7-phenyl-5-(trifluoromethyl)-pyrido[2,3-*d*] pyrimidin-2(1*H*)-thione **(2b)***

Yellow solid, yield: 64%, M.P.: 236–237 °C, IR: 3468, 3395, 3301, 3180, 1637, 1581, 1371, 1261, 1198, 1131 cm^{-1}; ^{1}H NMR (DMSO-d_6, 400 MHz) δ 6.30 (*s*, 2H, NH$_2$), 7.46–7.51 (m, 3H, Ar–H), 7.77 (*s*, 1H, NH), 8.06–8.10 (*m*, 3H, Ar–H) ppm; ^{13}C NMR (DMSO-d_6, 100 MHz) δ 104.8, 113.3, 121.4, 126.6, 128.8, 129.9, 135.4, 137.9, 155.6, 156.8, 166.6 ppm; MS (ESI): *m/z* (%) = 323.1 (15) $[M + H]^+$, 280.1 (100) $[M^+ - 42]$. Elemental analysis: calcd. For $C_{14}H_9F_3N_4S$: C, 52.17; H, 2.81; N, 17.38%. Found: C, 52.12; H, 2.87; N, 17.44%.

*4-Amino-7-phenyl-5-(trifluoromethyl)-pyrido[2,3-*d*] pyrimidin-2(1*H*)-one **(2c)***

White solid, yield: 68%, M.P.: 267–269 °C, IR: 3467, 3395, 3302, 3178, 1637, 1370, 1198, 1133 cm^{-1}; ^{1}H NMR (DMSO-d_6, 400 MHz) δ 6.29 (*s*, 2H, NH$_2$), 7.45–7.51 (*m*, 3H, Ar–H), 7.77 (*s*, 1H, NH), 8.06–8.09 (*m*, 3H, Ar–H) ppm; ^{13}C NMR (DMSO-d_6, 100 MHz) δ 103.6, 113.3, 121.6, 126.6, 128.6, 129.5, 135.1, 137.5, 155.6, 156.4, 166.6 ppm; MS (ESI): *m/z* (%) = 307.1 (15) $[M + H]^+$, 264.1 (100) $[M^+ - 42]$. Elemental analysis: calcd. For $C_{14}H_9F_3N_4O$: C, 54.91; H, 2.96; N, 18.29%. Found: C, 54.85; H, 2.99; N, 18.22%.

General procedure for the synthesis of 2-Amino-3-carboxamido-4-trifluoromethyl-6-phenyl pyridine (3)

It was prepared by following the reported method (Bhalerao and Krishnaiah 1995).

General procedure for the synthesis of 7-Phenyl-5-(trifluoromethyl)-pyrido[2,3-*d*]pyrimidin-2,4(1*H*, 3*H*)-dione (4)

A solution of triethylamine (0.218 g, 2.16 mmol) in anhydrous tetrahydrofuran (3 mL) was added dropwise to a mixture of **3** (0.258 g, 0.92 mmol) and triphosgene (0.106 g, 0.36 mmol) in anhydrous tetrahydrofuran (20 mL). The mixture was heated under reflux for 4 h, then cooled to room temperature and poured on to crushed ice. The solid separated was collected by filtration and washed with water. The crude product was dried and purified through column of silica gel (60–120 mesh) using *n*-hexane/ethyl acetate (4:1).

Pale yellow, yield: 68%, M.P.: > 300 °C, IR: 3267, 3132, 3053, 2847, 1739, 1694, 1595, 1570, 1402, 1368, 1130 cm^{-1}; ^1H NMR (DMSO-d_6, 400 MHz) δ 7.53–7.55 (*m*, 3H, Ar–H), 7.89 (*s*, 1H, Ar–H), 8.13–8.16 (*m*, 2H, Ar–H), 11.55 (*s*, 1H, NH), 11.92 (*s*, 1H, NH) ppm; ^{13}C NMR (DMSO-d_6, 100 MHz) δ 104.62, 112.65, 123.49, 127.59, 128.98, 131.36, 135.76, 137.74, 149.87, 154.35, 159.4, 160.98 ppm; MS (ESI): *m/z* (%) = 308.1 (100) $[M + H]^+$, 264.1 (78) $[M - 43]^+$. Elemental analysis: calcd. For $C_{14}H_8F_3N_3O_2$: C, 54.73; H, 2.62; N, 13.68%. Found: C, 54.79; H, 2.68; N, 13.61%.

General procedure for the synthesis of 3-(4,5-Dihydro-1*H*-imidazol-2-yl)-6-phenyl-4-(trifluoromethyl)pyridin-2-amine (5)

A mixture of compound **1** (1.052 g, 4 mmol), ethylenediamine (0.96 g, 16 mmol) and sulfur (0.032 g, 1 mmol) was heated under reflux on an oil bath (120 °C) for 4 h. The progress of the reaction was monitored by TLC (EtOAc/MeOH, 4:1). After completion of the reaction, the mixture was cooled to room temperature and cold water was added and extracted with chloroform. The organic layer was dried over anhydrous Na_2SO_4 and evaporated under reduced pressure. The residue obtained was recrystallized using cyclohexane.

Yellow solids, yield: 74%, M.P.: 232–234 °C, IR: 3473, 3346, 3180, 2931, 2864, 1625, 1582, 1497, 1373, 1267, 1133 cm^{-1}; ^1H NMR($CDCl_3$, 400 MHz) δ 3.75 (*m*, 4H, $2CH_2$), 5.77 (*s*, 2H, NH_2), 7.19 (*s*, 1H, NH), 7.24 (*s*, 1H, Ar–H), 7.41 (*m*, 3H, Ar–H), 7.90 (*m*, 2H, Ar–H) ppm; ^{13}C NMR ($CDCl_3$, 100 MHz) δ 25.05, 28.12, 104.48, 112.61, 120.63, 126.20, 127.43, 128.79, 136.81, 137.13, 156.92, 157.02, 160.07 ppm; MS (ESI): *m/z* (%) = 307.1 (100) $[M + H]^+$. Elemental analysis: calcd. For $C_{15}H_{13}F_3N_4$: C, 58.82; H, 4.28; N, 18.29%. Found: C, 58.77; H, 4.35; N, 18.23%.

General procedure for the synthesis of compounds (6a–b)

A mixture of compound **5** (1.53 g, 5 mmol) and triethylorthoformate/triethylorthoacetate (15 mL) was heated under reflux for 3 h. After cooling, the reaction mixture was poured on to cold water. The solid product was isolated by filtration, washed with water, dried, and crystallized using cyclohexane.

8-Phenyl-10-(trifluoromethyl)-2,3-dihydroimidazo[1,2-c]pyrido[3,2-e]pyrimidine ***(6a)***

White solid, yield: 61%, M.P.: 262–263 °C, IR: 1632, 1560, 1463, 1361, 1198, 1148, 1115 cm^{-1}; ^1H NMR ($CDCl_3$, 400 MHz) δ 4.08–4.13 (*m*, 2H, CH_2), 4.24–4.29 (*m*, 2H, CH_2), 7.49–7.52 (*m*, 3H, Ar–H), 8.01–8.03 (*m*, 2H, Ar–H), 8.16–8.19 (*m*, 2H, Ar–H) ppm; MS (ESI): *m/z* (%) = 339.4 (100) $[M + Na^+]^+$, 317.4 (65) $[M + H]^+$. Elemental analysis: calcd. For $C_{16}H_{11}F_3N_4$: C, 60.76; H, 3.51; N, 17.71%. Found: C, 60.81; H, 3.58; N, 17.66%.

5-Methyl-8-phenyl-10-(trifluoromethyl)-2,3-dihydroimidazo[1,2-c]pyrido[3,2-e]pyrimidine ***(6b)***

White solid, yield: 52%, M.P.: 282–283 °C, IR: 1633, 1561, 1467, 1304, 1265, 1129 cm^{-1}; ^1H NMR ($CDCl_3$, 400 MHz) δ 2.64 (*s*, 3H, CH_3), 4.14 (*t*, 2H, CH_2), 4.31 (*t*, 2H, CH_2), 7.47–7.51 (*m*, 3H, Ar–H), 7.83 (*s*, 1H, Ar–H), 8.11 (*m*, 2H, Ar–H) ppm; MS (ESI): *m/z* (%) = 353.1 (100) $[M + Na^+]^+$, 331.1 (65) $[M + H]^+$. Elemental analysis: calcd. For $C_{17}H_{13}F_3N_4$: C, 61.82; H, 3.97; N, 16.96%. Found: C, 61.89; H, 3.91; N, 16.88%.

X-ray crystallographic study of the precursor compound (1)

The intensities were corrected for *Lorentz* and polarization effects, and a multi-scan absorption correction was also performed. The structure was solved by direct methods using SHELXS97 (Sheldrick 1997), which revealed the positions of all non-hydrogen atoms. The non-hydrogen atoms were refined anisotropically. All of the hydrogen atoms were fixed at geometrically calculated positions and each was assigned a fixed isotropic displacement parameter with a value equal to 1.2 U_{eq} of its parent atom. They were riding with their bonded atoms. A weighting scheme of the form $w = 1/[\sigma^2(F_0^2) + (ap)^2 + bp]$ with $a = 0.0291$ and $b = 0.0$ was used. The refinement converged to a final *R* value of 0.0438 (wR2 = 0.0810 for 2276 reflections, $[I > 2\sigma(I)]$. The final difference map was featureless. The data collection and refinement parameters are given in supporting information.

Biological activity

Binding at human A_1, A_{2A} and A_3 ARs

Binding studies at hA_1, hA_{2A}, and hA_3 ARs were carried out by employing our previously reported procedures (Klotz et al. 1998). Chinese hamster ovary (CHO) cells stably transfected with human (h) A_1, A_{2A}, and A_3 ARs subtypes were used for the preparation of membranes for radioligand binding studies. Further, 1 nM [^{3}H]-2-chloro-6-cyclopentyl adenosine ([^{3}H]CCPA), 10 nM [^{3}H]-5'-*N*-ethylcarboxamido adenosine ([^{3}H]NECA) and 1 nM [^{3}H]-2-(1-hexynyl)-N^6-methyl adenosine ([^{3}H]HEMADO) were used as radioligands at the hA_1, hA_{2A} and hA_3 Ars, respectively. Nonspecific binding of [^{3}H]CCPA was determined in presence of 1 mM theophylline, while 100 µM (R)-N^6-phenyliso-propyladenosine (R-PIA) was used for [^{3}H]NECA and

[^{3}H]HEMADO, respectively (Klotz et al. 2007). Calculation of *K*i values from competition experiments was carried out by using the program SCIFIT (Delean et al. 1982).

Adenylyl cyclase activity

Due to the lack of a high affinity radioligand for A_{2B} AR adenylyl cyclase experiments were carried out as a measure of affinity for hA_{2B} AR by employing previously reported procedures with minor modifications (Klotz et al. 1985, 1998). Membranes were prepared from CHO cells stably transfected with hA_{2B} ARs followed by incubation with 100 nM NECA as well as 150,000 cpm of [α-^{32}P] ATP. All the target compounds were tested at different concentration for 20 min in the incubation mixture without using EGTA (ethylene glycoltetraacetic acid) and NaCl (Klotz et al. 1985). None of the compounds showed measureable interaction with the hA_{2B} AR (IC_{50} values > 90 µM; data not shown).

Results and discussion

Chemistry

The required precursor (**1**) was synthesized following an earlier reported protocol (Narsaiah et al. 1993, 1994). As shown in Scheme 1, the precursor **1** (2-amino-3-cyano-4-trifluoromethyl-6-phenyl-pyridine) on a cyclocondensation reaction with guanidine/thiourea/urea under basic conditions (sodium ethoxide) resulted in the formation of substituted pyrido[2,3-*d*]pyrimidines (**2a–c**). When these reactions were carried out in the absence of a base, the product formation was not observed. This could be due to the low nucleophilicity of 2-amino group of the precursor which may be attributed to two possibilities: the presence of a highly electron-withdrawing nitrile group in *ortho* position to the amino group and the distinct possibility of imine formation between the amino group and pyridine ring nitrogen due to tautomerism. Thus, nucleophilicity of the amino group in precursor is less when compared with aromatic amines. The complete disappearance of the nitrile absorption band at 2216 cm^{-1} in the IR spectra of **2a–c** indicated the utilization of the α-aminonitrile (**1**). The presence of amino groups at δ 6.27 ppm (C-4 NH_2) and 7.75–8.04 ppm (NH) in the ^{1}H NMR spectra of **2a–c** further confirmed the cyclization. The presence of a pyrimidine ring system was further confirmed by D_2O exchange of amino protons along with the presence of carbon signals at 156.41–166.67 ppm in ^{13}C NMR spectra. The formation of **2a–c** indicated that 2-amino group was actively participating in the nucleophilic attack with the selected reagents (guanidine/thiourea/urea). Further, it also provided an

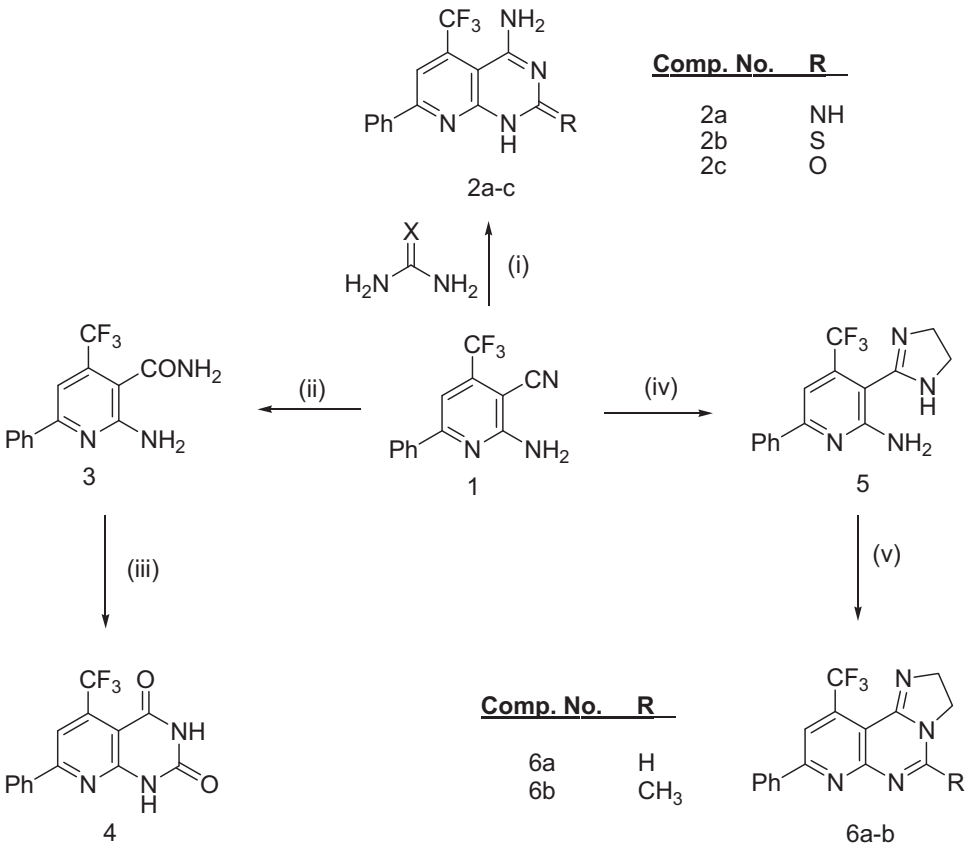

Scheme 1 Synthesis of substituted and heterofused pyrido[2,3-*d*]pyrimidines. Reagent and conditions: (i) guanidine/thiourea/urea, C_2H_5ONa/EtOH, reflux 48–50 h; (ii) KOH, reflux, 4 h; (iii) triphosgene, triethylamine/tetrahydrofuran, reflux; (iv) ethylenediamine, sulfur, 120 °C, 4 h; (v) triethylorthoformate/triethylorthoacetate, reflux 3 h

interesting clue that the nucleophilicity of the 2-amino group could be the rate limiting factor in these reactions.

Pyrido[2,3-*d*]pyrimidine analogue **4** was obtained by the cyclization of an intermediate 2-amino-3-carboxamido-4-trifluoromethyl-6-phenylpyridine **3** (Bhalerao and Krishnaiah 1995) using triphosgene in the presence of basic medium (triethylamine). The carbonyl group showed a strong signal at 1694 cm^{-1} in its IR spectrum and the ^1H NMR spectrum exhibited two signals at δ 11.55 ppm and δ 11.92 ppm corresponding to two NH protons. Further, fused pyrido[2,3-*d*]pyrimidines (**6a** and **6b**) were obtained by the cyclization of 3-(4,5-dihydro-1*H*-imidazol-2-yl)-6-phenyl-4-(trifluoromethyl)pyridin-2-amine (**5**) a new intermediate with one carbon donor reagents like triethylorthoformate/triethylorthoacetate. The intermediate **5** was synthesized by the functional conversion of cyano group in **1** to an imidazoline group by using 1,2-ethylene- diamine in the presence of sulfur as a catalyst. The IR spectrum of compound **5** showed disappearance of C≡N stretch and an absorption band at 3180 cm^{-1} related to the N–H stretch. Its ^1H NMR spectrum showed a multiplet signal at δ 3.75 ppm for methylene protons and a singlet at δ 7.19 ppm corresponding to the imidazoline –NH. The IR and ^1H NMR spectra of **6a–b** showed the absence of characteristic absorption bands for primary and secondary amino groups which authenticated the formation of cyclized compounds. The conversion of cyano to other groups (carboxamido or imidazolino) improved the nucleophilicity of the amino group of the compound **5** as compared to the precursor (**1**), facilitating subsequent convenient cyclization reaction under mild conditions to result in the formation of fused-pyrimidine analogues.

X-ray diffraction analysis of compound 1

To explore the versatility of this precursor compound (**1**), a crystallization process with various solvents was attempted. Interestingly, distinct monoclinic crystals were obtained when absolute ethanol was used as a crystallizing solvent. It prompted us to investigate further its X-ray crystallographic data to understand the reactivity of this key intermediate towards a variety of reagents. Compound **1** crystallizes in a monoclinic crystal system (space group = $P2_1/c$) with four molecules in the unit cell. A perspective view of the molecule with numbering scheme is shown in Fig. 3.

All the bond lengths and angles observed in the structure are normal. The cyano group, as expected, is almost linear with a C2-C7-N3 angle of 177.8 (2)°. The trifluoromethyl group orients with the pyridyl ring in such a fashion that there is a short contact of 2.391 Å between one of the fluorine atoms and the adjacent hydrogen (F2…H4A = 2.391 Å, C4-H4A… F2 = 100.08°) which can be considered as in intramolecular C–H…F interaction.

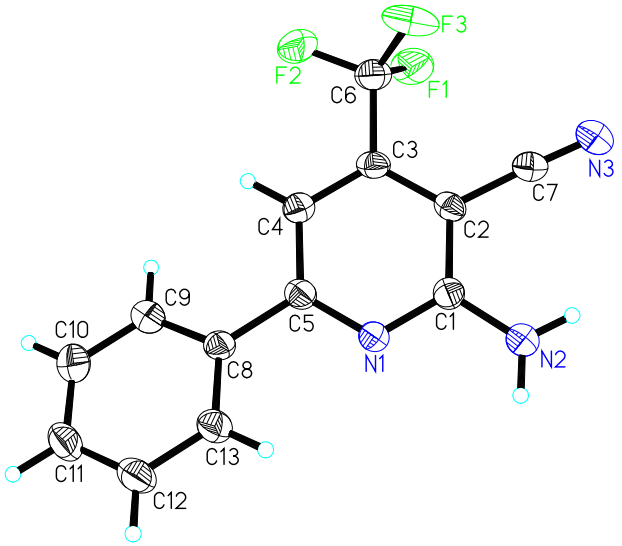

Fig. 3 An ORTEP view of compound **1** with atom numbering scheme employed

One of the noteworthy features in the molecular structure of **1** is the near planar orientation of the phenyl group with the pyridyl ring, the torsional angle N1-C5-C8-C13 is only 18.6°, even though there can be complete flexibility in rotation of C5-C8 bond. The cause for such an orientation is two-fold, the better resonance stabilization as the two aromatic rings become co-planar and the structure stabilization through an intramolecular C–H···N hydrogen bonding between N1 and one of the *ortho* hydrogen atoms (H13A) of the phenyl ring (N1…H13A = 2.509 Å, C13-H13A…N1 = 99.6°). In the crystal lattice, molecules are packed in a herringbone manner as shown in Fig. 4. In the wedge shape region of the herringbone two molecules form a centrosymmetric dimer through a pair of N–H…N hydrogen bonds (N3…H2B = 2.212 Å, N2-H2B…N3 = 160.01°) between the adjacent $–NH_2$ and –CN functionality (Fig. 5a). Further, these dimers stack one over the other through a sheared manner (Fig. 5b) in which the pyridyl and phenyl rings are 3.84 Å apart that shows π…π stacking interactions between the aromatic moieties. There are no other short contacts observed in the crystal lattice.

The observed coplanarity of the two rings (phenyl and pyridyl) of the precursor might have contributed towards its improved reactivity of both amino and nitrile groups located on the pyridine ring. This could probably be the reason why several reactions on nitrile and amino groups individually as well as together in one step have been successfully conducted. Our observation of the quantitative yields with such condensations using appropriate reagents is noteworthy. Earlier, we reported reactions involving pyridopyrimidine system with low to moderate yields (Suma et al. 2000). Now, it can be understood that the strategically located

phenyl substituent at 6-position of pyridine nucleus could perhaps be responsible for these unexpectedly high yields of these type of reactions. The fluorinated fused quinazolines (**17a–c** and **18a–c**) were synthesized and characterized as per our earlier report (Balakumar et al. 2010) by following the synthetic route as shown in Scheme 2.

Biological activity

All the newly synthesised fluorinated pyrido[2,3-*d*]pyrimidines (**2a–c, 4** and **6a–b**) and previously reported fluorinated quinazolines (**17a–c** and **18a–c**) were evaluated for their binding affinity and selectivity towards hA_1, A_{2A}, A_{2B}, and A_3 ARs which were expressed in CHO cells. Three different radioligands such as [^{3}H]CCPA, [^{3}H]NECA, and [^{3}H]HEMADO were used for hA_1, hA_{2A}, and hA_3 ARs, respectively. The AR binding affinity and selectivity data of compounds **2a–c, 4** and **6a–b** are provided in Table 1. A potential agonistic activity of these compounds towards hA_{2B} AR was investigated by measuring adenylyl cyclyse activity, while the amount of inhibition of NECA-stimulated adenylyl cyclase activity would provide a measurement of an antagonistic nature. Interestingly, none of these compounds showed detectable interaction with the hA_{2B} AR (data not shown in Table 1) in an agonistic or antagonistic fashion (EC_{50} or IC_{50} values > 90 μM).

In the series of fluorinated pyrido[2,3-*d*]pyrimidines (**2a–c** and **4**), compound **2a** exhibited the maximum binding affinity for hA_3 AR with similar affinity for the hA_1 and somewhat lower affinity for hA_{2A} ARs resulting in a compound with no A_3 selectivity vs. A_1 and moderate selectivity vs. A_{2A} AR (K_i $hA_1 = 0.62$ μM, $hA_{2A} = 3.59$ μM and $hA_3 = 0.42$ μM). This could be attributed to the presence of free amino group at 2-position of pyrido[2,3-*d*]pyrimidine nucleus in addition to amino group at 4-position of the scaffold. Replacement of the free amino (NH_2) group with sulphur or oxygen atom in 2-position of the pyrimidine moiety of compounds **2b** and **2c** drastically lowered the affinity for all the AR subtypes. Interestingly, in case of compound **4**, the presence of a carbonyl (C=O) group at 2-position and 4-position of the pyrimidine moiety improved the affinity for hA_1 AR but showed poor selectivity against hA_{2A} and hA_3 ARs (K_i $hA_1 = 0.17$ μM, $hA_{2A} = 0.67$ μM and $hA_3 = 0.68$ μM). The fusion of an imidazole ring with the pyrimido moiety of the scaffold in case of compounds **6a** and **6b** further showed detrimental effect on the affinity for all the ARs.

There are numerous examples of more potent antagonists for A_1, A_{2A}, and A_3AR (Fredholm et al. 2001, 2011), however, many structurally novel compounds show affinities in the low micromolar or high nanomolar range (Cagide et al. 2015). Although further development of such ligands is usually aiming at improved affinity this is not essential as many successfully used drugs show affinities in this range such as Ranitidine (0.20 μM) and Loratadine (0.16 μM) (Hill et al. 1997).

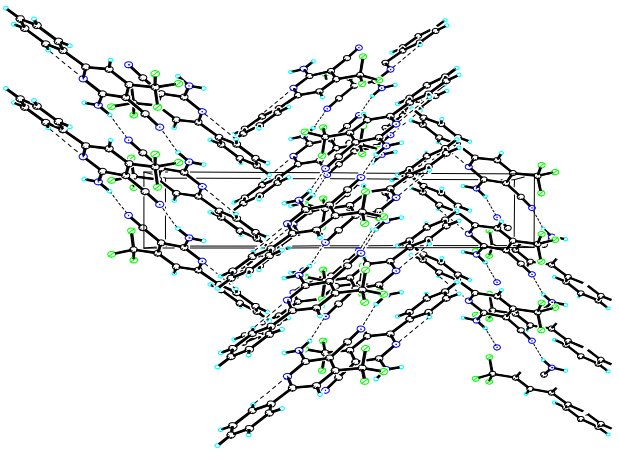

Fig. 4 Packing of 1 viewed down a axis showing the herring-bone arrangement of molecules in the crystal lattice. The dimer formation through N–H…N hydrogen bonds are shown as dashed lines

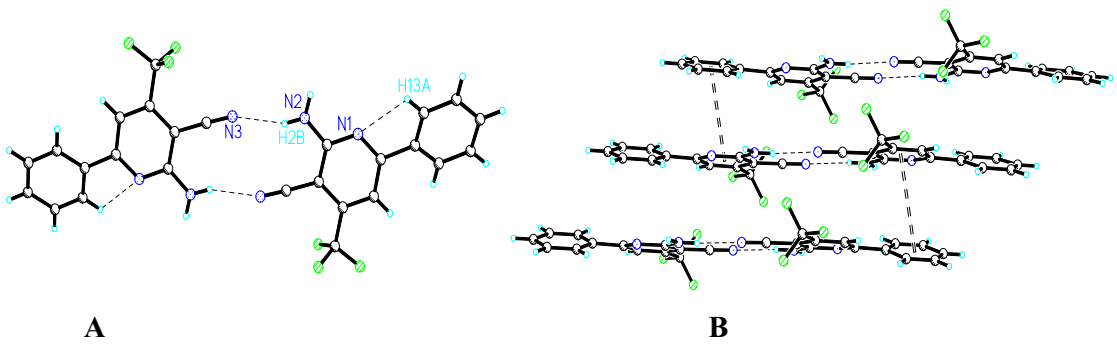

Fig. 5 **a** The dimer formation through N–H…N hydrogen bonding (dashed line) in **1**. The dashed solid line shows the π…π interaction between the pyridyl andphenyl moieties. **b** The stacking pattern of **1**. The dashed solid line shows π…π interaction between the pyridyl and phenyl moieties

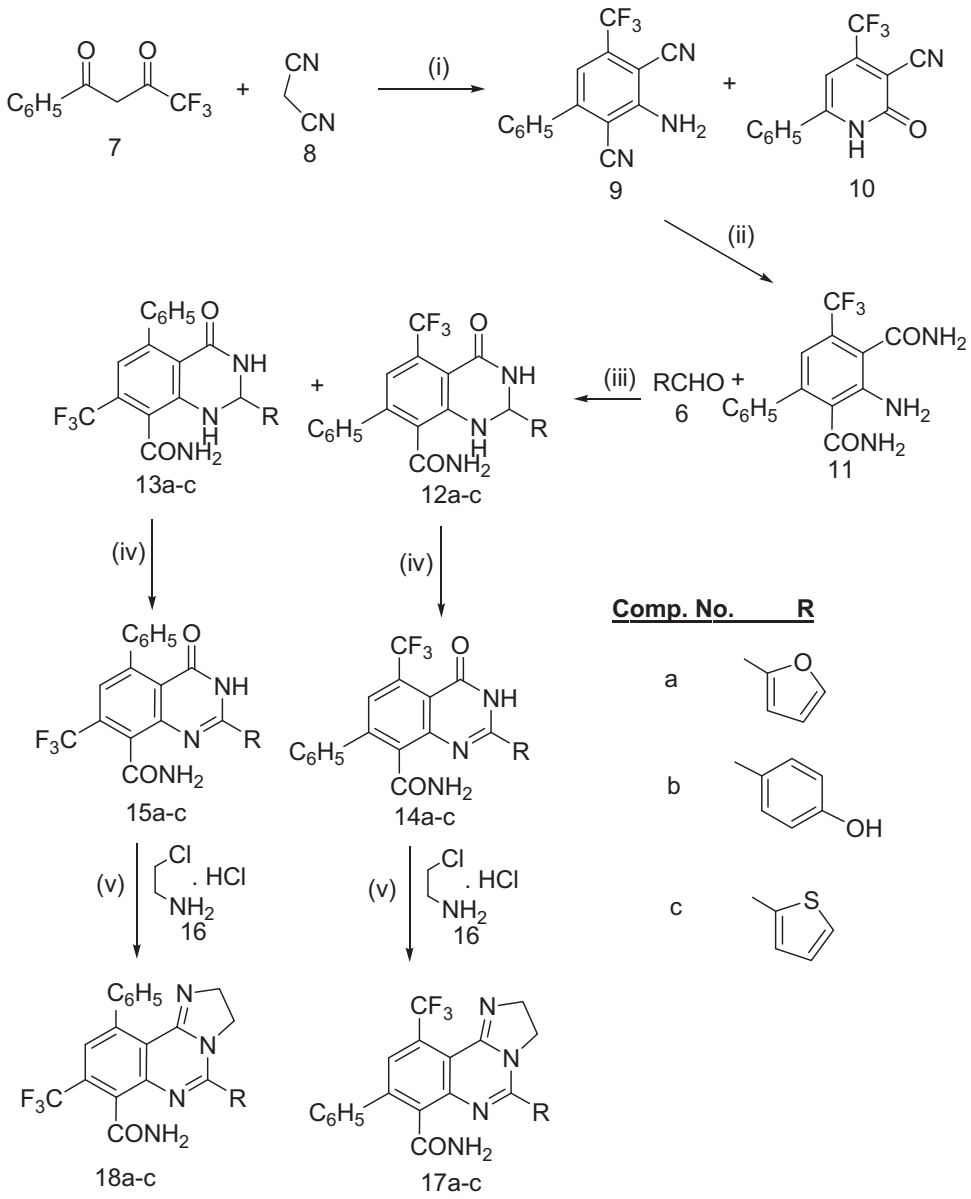

Scheme 2 Synthesis of fluorinated quinazolines. Reagents and conditions: (i) methanol, reflux, 6 h; (ii) 20% KOH, reflux, 7 h; (iii) glacial acetic acid, r.t., 4 h; (iv) MnO_2, dichloromethane, r.t., 2 h; (v) $POCl_3$, reflux, 5 h (Balakumar et al. 2010)

In the quinazoline series, compound **18a** was found to be the most active with substantial binding affinity for A_1 AR as well as significant selectivity against A_{2A} and A_3 ARs (K_i $hA_1 = 0.73\ \mu M$, $hA_{2A} > 30\ \mu M$ and $hA_3 = 9.27\ \mu M$). Surprisingly, other quinazoline derivatives (**17a–c, 18b** and **18c**) did not show remarkable affinity for any of the AR subtypes.

Conclusion

In conclusion, we have synthesized and characterised some new fluorinated pyrido[2,3-*d*]pyrimidines (**2a–c** and **4**) and fluorinated imidazo[1,2-*c*]pyrido[3,2-*e*]pyrimidines (**6a–b**) in quantitative yields by using 2-amino-4-trifluoromethyl-6-phenyl nicotinonitrile (**1**) as a precursor following an appropriate synthetic Scheme 1. In order to gain insight into the structural features as well as to illustrate the reactivity of the key precursor (**1**), we also examined the X-ray crystal structure. Further, a series of fluorinated heterofused quinazolines (**17a–c** and **18a–c**) were also synthesized and characterized as they are bioisosteres to pyrido[2,3-*d*]pyrimidines based on our earlier report. Radioligand binding affinity studies of all these compounds for ARs showed that pyrido[2,3-*d*]pyrimidine scaffold with free amino (NH_2) group at 2-position and 4-position (compound **2a**) exhibited good binding affinity for hA_3 AR with no selectivity against hA_1, but moderate hA_{2A} selectivity. Interestingly, the

Table 1 Binding affinity (K_i) of compounds (**2a–c**, 4, **6a–b**, **17a–c** and **18a–c**) at hA_1, $hA_{2A,}$ and hA_3 ARs and selectivity against hA_1 and hA_{2A} ARs

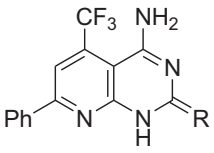

2a-c

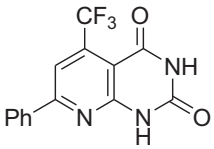

4

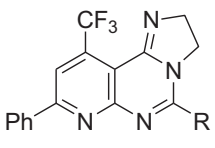

6a-b

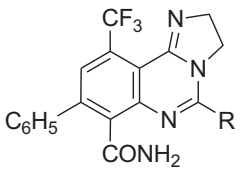

17a-c

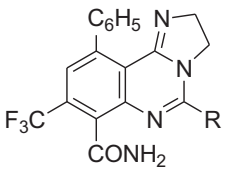

18a-c

CN	R	K_i, μM (95 % Cl)			Selectivity		
		hA_1[a]	hA_{2A}[b]	hA_3[c]	hA_1/hA_{2A}	hA_1/hA_3	hA_{2A}/hA_3
2a	NH_2	0.623 (0.561–0.692)	3.59 (1.76–7.33)	0.429 (0.310–0.595)	0.17	1.5	8.4
2b	S	12.9 (7.52–22.1)	>30	5.85 (3.45–9.91)	>0.43	2.2	>5.1
2c	O	11.1 (6.16–19.9)	>30	19.5 (10.3–37.2)	>0.37	0.57	>1.5
4	–	0.176 (0.161–0.192)	0.678 (0.469–0.980)	0.685 (0.444–1.06)	0.26	0.26	0.99
6a	H	3.08 (1.65–5.73)	7.03 (6.36–7.77)	3.19 (2.43–4.18)	0.44	0.96	2.2
6b	CH_3	>30	27.3 (22.1–33.7)	13.40 (8.43–21.4)	>1	2.2	2.0
17a		5.84 (4.69–7.27)	22.6 (14.4–35.2)	2.34 (1.42–3.87)	0.25	2.5	9.7
18a		0.73 (0.65–0.82)	>30	9.27 (4.71–18.3)	0.02	0.07	3.2
17b	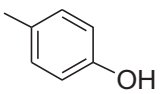	7.80 (6.81–8.94)	24.5 (17.0–35.3)	2.52 (1.25–5.09)	0.31	3.09	9.7
18b	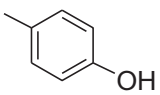	2.57 (1.35–4.91)	8.62 (4.86–15.3)	3.96 (3.16–4.97)	0.29	0.64	2.2
17c		10.6 (7.72–14.4)	26.0 (22.5–30.1)	3.85 (3.09–4.78)	0.40	2.8	6.8
18c		1.97 (1.77–2.19)	6.62 (4.49–9.76)	1.87 (1.23–2.82)	0.29	1.05	3.5

Data are expressed as geometric means, with 95% confidence limits in parentheses

[a] Displacement of specific [^{3}H]CCPA binding at human A_1 AR expressed in CHO cells (n = 3–6)

[b] Displacement of specific [^{3}H]NECA binding at human A_{2A} AR expressed in CHO cells (n = 3–6)

[c] Displacement of specific [^{3}H]HEMADO binding at human A_3 AR expressed in CHO cells (n = 3–6)

replacement of both the amino groups with carbonyl (C=O) groups (compound **4**) resulted in significantly improved affinity for hA_1 AR but with moderate selectivity against hA_{2A} and hA_3 ARs. Further, fusion of an imidazole ring with the pyrimidine moiety of the scaffold (compounds **6a** and **6b**) showed detrimental effect in affinity for all the ARs. In case of fluorinated quinazolines, only compound **18a** showed good affinity for hA_1 AR with significant selectivity against hA_{2A} and hA_3 ARs. The preliminary result of these compounds demonstrate that the fluorinated pyrido[2,3-*d*]pyrimidine and imidazo[1,2-*c*]pyrido[3,2-*e*] pyrimidine can be considered as promising scaffolds for further optimisation in search of potential antagonists with better affinity and selectivity towards hA_1 and hA_3 ARs.

Acknowledgements We thank Mr. Raveesh Sankolli, IISc, Bangaluru for providing the X-ray structural data. One of the authors (CB) is grateful to University Grants Commission (UGC), New Delhi for providing research fellowship [UGC-RFSMS; Grant No. F.4-1/2006 (XI Plan/BSR)]. This work was also supported by AICTE, New Delhi through a grant to ARR under Research Promotion Scheme (RPS-8023/2006-07).

Compliance with ethical standards

Conflict of interest The authors declare that they have no competing interests.

References

Bahreyni A, Samani SS, Khazaei M, Ryzhikov M, Avan A, Hassanian SM (2017) Therapeutic potentials of adenosine receptors agonists and antagonists in colitis; Current status and perspectives. J Cell Physiol https://doi.org/10.1002/jcp.26073.

Balakumar C, Lamba P, Pran Kishore D, Lakshminarayana B, Venkat Rao K, Rajwinder K, Raghuram Rao A, Shireesha B, Narsaiah B (2010) Synthesis, anti-inflammatory evaluation and docking studies of some new fluorinated fused quinazolines. Eur J Med Chem 45:4904–4913

Balakumar C, Pran Kishore D, Venkat Rao K, Lakshminarayana B, Rajwinder K, Rajkumar V, Raghuram Rao A (2012) Design, microwave-assisted synthesis and *in silic*o docking studies of new *4*H-pyrimido[2,1-b]benzothiazole-2-arylamino-3-cyano-4-ones as possible adenosine A_{2B} receptor antagonists. Indian J Chem 51B:1105–1113

Balakumar C, Pran Kishore D, Raghuram Rao A (2017) Structure-based design and pharmacological study of fluorinated fused quinazolines as adenosine A_{2B} receptor antagonists. JSM Chem 5 (2):1041

Baraldi PG, Mojgan AT, Gessi S, Borea PA (2008) Adenosine receptor antagonists: translating medicinal chemistry and pharmacology into clinical utility. Chem Rev 108:238–263

Bertelli L, Biagi G, Giorgi I, Livi O, Manera C, Scartoni V, Lucacchini A, Giannaccini G, Barili PL (2000) Substituted 1,2,3-triazolo[1,5-*a*]quinazolines: synthesis and binding to benzodiazepine and adenosine receptors. Eur J Med Chem 35:333–341

Bhalerao UT, Krishnaiah A (1995) A mild and efficient method for the dehydrogenation of dihydropyridopyrimidinones and related compounds by using active MnO_2. Indian J Chem 34B:587–590

Borea PA, Gessi S, Bar-Yehuda S, Fishman P (2009) A_3 adenosine receptor: pharmacology and role in disease. Adenosine receptors in health and disease. Handb Exp Pharmacol 193:297–327

Brown RA, Spina D, Page C (2008) Adenosine receptors and asthma. Br J Pharmacol 153:S446–S556

Bulicz J, Bertarelli DC, Baumert D, Muller CE, Heber D (2006) Synthesis and pharmacology of pyrido[2,3-*d*]pyrimidinediones bearing polar substituents as adenosine receptor antagonists. Bioorg Med Chem 14:2837–2849

Burbiel JC, Ghattas W, Kuppers P, Kose M, Lacher S, Herzner AM, Kombu RS, Raghuram Rao A, Hockemeyer J, Muller CE (2016) 2-Amino[1,2,4]triazolo[1,5-*c*]quinazolines and derived novel heterocycles: syntheses and structure-activity relationships of potent adenosine receptor antagonists. Chem Med Chem 11:2272–2286

Cagide F, Gaspar A, Reis J, Chavarria D, Vilar S, Hripcsak G, Uriarte E, Kachler S, Klotz K-N, Borges F (2015) Navigating in chromone chemical space: disocvery of novel and distinct A3 adenosine receptor ligands. RSC Adv 5:78572–78585

Cosimelli B, Greco G, Laneri S, Novellino E, Sacchi A, Trincavelli ML, Giacomelli C, Taliani S, Settimo FD, Martini C (2016) 4-amino-6-alkyloxy-2-alkylthio pyrimidine derivatives as novel non-nucleoside agonists for the adenosine A_1 receptor. Chem Biol Drug Des 88:724–729

Delean A, Hancock A, Lefkowitz RJ (1982) Validation and statistical-analysis of a computer modeling method for quantitative-analysis of radioligand binding data for mixtures of pharmacological receptor subtypes. Mol Pharmacol 21:5–16

Dong G, Heitman LH, Adriaan PI (2017) Kinetic aspects of the interaction between ligand and g protein-coupled receptor: The case of the adenosine receptors. Chem Rev 117:38–66

Dungo R, Deeks ED (2013) Istradefylline: first global approval. Drugs 73:875–882

Eastwood P, Esteve C, González J, Fonquerna S, Aiguadé J, Carranco I, Doménech T, Aparici M, Miralpeix M, Albertí J, Córdoba M, Fernández R, Pont M, Godessart N, Prats N, Loza MI, Cadavid MI, Nueda A, Vidal B (2011) Discovery of LAS101057: a potent, selective, and orally efficacious A_{2B} adenosine receptor antagonist. ACS Med Chem Lett 2:213–218

Fredholm BB, IJzerman AP, Jacobson KA, Klotz K-N, Linden J (2001) International union of pharmacology. XXV. Nomenclature and classification of adenosine receptors. Pharmacol Rev 53:527–552

Fredholm BB, IJzerman AP, Jacobson KA, Linden J, Muller CE (2011) International union of basic and clinical pharmacology. LXXXI. Nomenclature and classification of adenosine rceptors-An update. Pharmacol Rev 63:1–34

Hafez HN, Abbas HA, El-Gazzar AR (2008) Synthesis and evaluation of analgesic, antiinflammatory and ulcerogenic activities of some triazolo- and 2-pyrazolyl-pyrido [2,3-*d*]pyrimidines. Acta Pharm 58:359–378

Hill SJ, Ganellin CR, Timmerman H, Schwartz JC, Shankley NP, Young JM, Schunack W, Levi R, Haas HL (1997) International union of pharmacology. XIII. Classification of histamine receptors. Pharmacol Rev 49:253–278

Jacobson KA, Klutz AM, Tosh DK, Ivanov AA, Preti D, Baraldi PG (2009) Medicinal chemistry of the A_3 adenosine receptor: agonists, antagonists, and receptor engineering. Handb Exp Pharmacol 193:123–159

Kalla RV, Zablocki J (2009) Progress in the discovery of selective, high affinity A_{2B} adenosine receptor antagonists as clinical candidates. Purinergic Signal 5:21–29

Kazemi MH, Raoofi MS, Hojjat-Farsangi M, Anvari E, Ghalamfarsa G, Mohammadi H, Jadidi- Niaragh F (2017) Adenosine and

adenosine receptors in the immunopathogenesis and treatment of cancer. J Cell Physiol https://doi.org/10.1002/Jcp.25873.

Khan I, Ibrar A, Abbas N, Saeed A (2014) Recent advances in the structural library of functionalized quinazoline and quinazolinone scaffolds: synthetic approaches and multifarious applications. Eur J Med Chem 76:193–244

Klotz K-N, Cristalli G, Grifantini M, Vittori S, Lohse MJ (1985) Photo affinity-labeling of A_1-adenosine receptors. J Biol Chem 260:4659–4664

Klotz K-N, Falgner N, Kachler S, Lambertucci C, Vittori S, Volpini R, Cristalli G (2007) [^{3}H]HEMADO - A novel highly potent and selective radiolabeled agonist for A_3 adenosine receptors. Eur J Pharmacol 556:14–18

Klotz K-N, Hessling J, Hegler J, Owman C, Kull B, Fredholm BB, Lohse MJ (1998) Comparative pharmacology of human adenosine receptor subtypes-characterization of stably transfected receptors in CHO cells. Naunyn Schmiedebergs Arch Pharmacol 357:1–9

Muller CE, Jacobson KA (2011) Recent developments in adenosine receptor ligands and their potential as novel drugs. Biochim Biophys Acta 1808:1290–1308

Nam G, Yoon CM, Kim E, Rhee CK, Kim JH, Shin JH, Kim SH (2001) Syntheses and evaluation of pyrido[2,3-*d*]pyrimidine-2,4-diones as PDE 4 inhibitors. Bioorg Med Chem Lett 11:611–614

Narsaiah B, Sivaprasad A, Venkataratnam RV (1993) An improved synthetic route to trifluoromethyl-6-substituted-2(1*H*)-pyridones. OPPI Briefs 25:116–117

Narsaiah B, Sivaprasad A, Venkataratnam RV (1994) A novel synthetic route to 2-amino-3-cyano-4-trifluoromethyl-6-substituted pyridines. J Fluorine Chem 67:87–90

Pran Kishore D, Balakumar C, Raghuram Rao A, Roy PR, Roy K (2011) QSAR of adenosine receptor antagonists: exploring physicochemical requirements for binding of pyrazolo[4,3-*e*]1,2,4-triazolo[1,5-*c*]pyrimidine derivatives with human adenosine A_3 receptor subtype. Bioorg Med Chem Lett 21:818–823

Preti D, Baraldi PG, Moorman AR, Borea PA, Varani K (2015) History and perspectives of A_{2A} adenosine receptor antagonists as potential therapeutic agents. Med Res Rev 35:790–848

Raghu Prasad M, Raghuram Rao A, Shanthan Rao A, Rajan KS, Meena S, Madhavi K (2008) Synthesis and adenosine receptor binding studies of some novel triazolothieno- pyrimidines. Eur J Med Chem 43:614–620

Ribeiro JA, Sebastiao AM, De Mendonca A (2002) Adenosine receptors in the nervous system: pathophysiological implications. Prog Neurobiol 68:377–392

Sheldrick GM (1997) SHELXS97, program for the solution of crystal structures. University of Gottingen, Gottingen (Germany)

Shook BC, Charavarty D, Barbay JK, Wang A, Leonard K, Alford V, Powell M, Beauchamp DA, Rassnick S, Scannevin R, Carroll K, Wallace N, Crooke J, Ault M, Lampron L, Westover L, Rhodes K, Jackson PF (2011) Aminomethyl substituted thieno [2,3-*d*] pyrimidines as adenosine A_{2A} receptor antagonists. Med Chem Commun 2:950–965

Smutny T, Nova A, Drechslerová M, Carazo A, Hyrsova L, Hrušková ZR, Kunes J, Pour M, Špulák M, Pavek P (2016) 2-(3-Methoxyphenyl)quinazoline derivatives: a new class of direct constitutive androstane receptor (CAR) agonists. J Med Chem 59:4601–4610

Suhagia BN, Chhabria MT, Makwana AG (2006) Design, synthesis and pharmacological screening of a series of N^1-(substituted) aryl-5,7-dimethyl-2-(substituted)pyrido[2,3-*d*]-pyrimidin-4(3*H*)-ones as potential histamine H_1-receptor antagonists. J Enzyme Inhib Med Chem 21:681–691

Suma G, Bahekar RH, Raghuram Rao A (2000) A facile method with improved yields in the synthesis of 6-arylpyrido[2′,3′:4,5]pyrimido[1,6-*a*]benzimidazoles. OPPI Briefs 32:99–101

van Rhee AM, Siddiqi SM, Melman N, Shi D, Padgett WL, Daly JW, Jacobson KA (1996) Tetrahydrobenzothiophenone derivatives as a novel class of adenosine receptor antagonists. J Med Chem 39:398–406

Venkatesan G, Paira P, Cheong SL, Vamsikrishna K, Federico S, Klotz K-N, Spalluto G, Pastorin G (2014) Discovery of simplified N^2-substituted pyrazolo[3,4-*d*]pyrimidine derivatives as novel adenosine receptor antagonists: efficient synthetic approaches, biological evaluations and molecular docking studies. Bioorg Med Chem 22:1751–1765

Veeraswamy B, Balakumar C, Meryem K, Christin V, Christa EM, Kurumurthy C, Santhoshkumar G, Sambasivarao P, Raghuprasad M, Raghuramarao A, Shanthanrao P, Narsaiah B (2013) Synthesis of novel pyrido[3,2-*e*][1, 2,4]triazolo[1,5-c]pyrimidine derivatives: potent and selective adenosine A_3 receptor antagonists. Arch Pharm 346:699–707

Wardas J, Konieczny J, Lorenc-Koci E (2001) SCH 58261, an A(2A) adenosine receptor antagonist, counteracts parkinsonian-like muscle rigidity in rats. Synapse 41:160–171